Analytical and numerical models of a bimorph mirror

A.S. Sobolev, T.Yu. Cherezova, and A.V. Kudryashov

Moscow State University

Received October 5, 2004

An improved analytical expression for the response function of a deformable semi-passive bimorph mirror is presented and compared with the experimentally measured response functions. Two numerical models simulating such a mirror, which are based on two approaches of the finite element method, are presented and compared.

Introduction

An adaptive mirror is a key element of many modern systems for control and correction of radiation. Moreover, the parameters of a system and the scope of the problems, it solves, are largely determined by the capabilities and peculiarities of the controllable optical element used. For the problems of correction for phase distortions of radiation and formation of preset intensity distribution, the optimal corrector is a flexible bimorph mirror.[1,2]

One of the principle requirements to the corrector is the possibility to introduce needed distortions into the phase of the incident radiation. Therefore, the main characteristic of any adaptive mirror is the response function of its actuators. As known, the response function of a mirror is a deformation of its surface upon the application of unit voltage to the control electrode. There is an analytical model of a bimorph mirror, based on obtaining an explicit solution to the equation of deformation of a mirror as a thin two-layer plate.[3–5] However, this model is too complicated for practical use, and it ignores geometric features of a flexible mirror (for example, spherical substrate or different diameters of a substrate and piezoceramics) and the difference in the Poisson coefficients of a substrate and ceramics. Therefore, it is needed to develop numerical models of a mirror with the allowance made for the above disadvantages of the analytical model.

The investigations of a bimorph mirror started from the paper by Kokorovsky,[3] who derived and solved the equation of mirror deformation for the case of a rectangular plate. The equation of deformation of a round plate with electrodes in the shape of segments was deduced and solved analytically in Refs. 4 and 5. Numerical solutions of this problem, suitable for practical use, have not been published.

In this paper, we present two numerical models of a mirror, constructed with the aid of two approaches of the finite element method (FEM). This method is widely used in calculating the elastically deformed state of various constructions,[6,7] in particular, those containing piezoceramic elements. However, in this paper it has been applied to calculation of a flexible mirror for the first time.

Optimization of the analytical equation

The typical design of a bimorph mirror, which is considered in this paper, is shown in Fig. 1*a*.

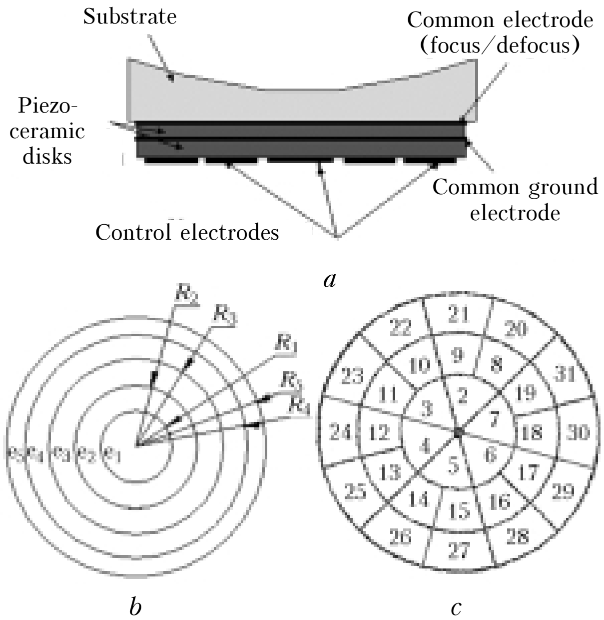

Fig. 1. Design of a flexible mirror (*a*); configuration of electrodes of a five-electrode mirror: e_1, e_2, e_3, e_4, e_5 are mirror electrodes with the radii $R_1 = 9$, $R_2 = 17$, $R_3 = 25$, $R_4 = 33$, $R_5 = 41$ mm, respectively (*b*); configuration of electrodes of a 30-electrode mirror (*c*). Each electrode is marked by the corresponding digit. The first electrode is common and serves for correction of defocus (*a*).

As known, the equation of mirror deformation can be represented in the following form[4,5]:

$$(\rho_1 h_1 + \rho_2 h_2) a^4 \frac{\partial^2 W(\mathbf{r},t)}{\partial t^2} + D\nabla^2\nabla^2 W(\mathbf{r},t) = \\ = \frac{d_{31} a^2 E_1 (2\Delta_1 k_1 - h_1^2)}{2(1-\nu)} \nabla^2 E_{el}(\mathbf{r},t) \quad (1)$$

with the boundary conditions:

$$\frac{\partial^2 W}{\partial \varphi^2} + \frac{1}{\nu - 1}\nabla^2 W + \frac{\partial W}{\partial r} = 0 \text{ at } r = 1, \quad (1a)$$

 © 2005 Institute of Atmospheric Optics

$$\frac{\partial\nabla^2 W}{\partial r} + (\nu - 1)\frac{\partial}{\partial r}\left(\frac{1}{r}\frac{\partial^2 W}{\partial\varphi^2}\right) = 0 \text{ at } r = 1, \qquad (1b)$$

where

$$D = \frac{E_2}{1-\nu^2}\left(\frac{\Delta_1^3}{3} + \frac{\Delta_2^3}{3} - \Delta_1^2 h_1 + \Delta_1 h_1^2 - \frac{h_1^3}{3}\right) + \frac{E_1}{1-\nu^2}\left(\Delta_1^2 h_1 - \Delta_1 h_1^2 + \frac{h_1^3}{3}\right)$$

is the cylindrical stiffness of the plate;

$$\Delta_2 = \frac{E_2 h_2^2 + E_1(h^2 - h_2^2)}{2(E_2 h_2 + E_1 h_1)}, \quad \Delta_1 = h - \Delta_2$$

are the distances from the median plane to the ceramics and substrate edges; $E_{el}(\mathbf{r}, t)$ is the electric field, applied to the piezoceramics; $W(\mathbf{r}, t)$ is the shift of the plate surface, $\mathbf{r} = \{r,\varphi\}$, t are the polar coordinates in the plate plane and time, the dimensionless coordinate $r = \rho/a$ is normalized to the plate radius a; $E_{1,2}$, $\rho_{1,2}$, $h_{1,2}$ are the Young's modulus, density, and thickness of the ceramics and substrate, respectively; d_{31} is the transverse piezoelectric modulus of the ceramics; ν is the Poisson coefficient, which is taken to be the same for the ceramics and substrate. The boundary conditions in the form (1a), (1b) mean the free fixing of the plate, which allows the maximum amplitude of deformations to be attained.

We have obtained a refined analytical solution to the equation of mirror deformation as compared to the solutions published earlier.[4,5] This equation accounts for the dependence of the electrode response function on the geometric dimensions of the electrode (in the case of segmented electrodes, segment coordinates r_1, r_2 and polar angles θ_1, θ_2) and on the plate density in the static case. The refined expression for the response function at the frequency p is explicitly described by the following equation:

$$W(r,\theta,p) = M[W_{ncs}(r,\theta,p) + W_{cs}(r,p)], \qquad (2)$$

$$W_{ncs}(r,\theta,p) = M\sum_{\substack{n=1\\k=0}}^{\infty}\frac{\Phi_{nk}(r)\cos n\theta}{p^2 - \omega_{nk}^2}\times$$

$$\times\left\{\left[\Phi'_{nk}(r_2)r_2 - \Phi'_{nk}(r_1)r_1\right]\frac{1}{n}\left[\sin(n\theta_2) - \sin(n\theta_1)\right] + \int_{r_2}^{r_1}\frac{\Phi_{nk}(\rho)}{\rho}d\rho n\left[\sin(n\theta_1) - \sin(n\theta_2)\right]\right\} +$$

$$+ M\sum_{\substack{n=1\\k=0}}^{\infty}\frac{\Phi_{nk}(r)\sin n\theta}{p^2 - \omega_{nk}^2}\left\{\left[\Phi'_{nk}(r_2)r_2 - \Phi'_{nk}(r_1)r_1\right]\times\frac{1}{n}[\cos(n\theta_1) - \cos(n\theta_2)] + \int_{r_2}^{r_1}\frac{\Phi_{nk}(\rho)}{\rho}d\rho n\left[\cos(n\theta_2) - \cos(n\theta_1)\right]\right\},$$

$$W_{cs} = \sum_{k=0}^{\infty}\frac{\Phi_{0k}(r)(\theta_2 - \theta_1)}{p^2 - \omega_{0k}^2}\left[\Phi'_{0k}(r_2)r_2 - \Phi'_{0k}(r_1)r_1\right];$$

$$M(r,\varphi) = \frac{d_{31}E_1(2\Delta_1 h_1 - h_1^2)}{2(1-\nu)a^2(\rho_1 h_1 + \rho_2 h_2)}E_{el}(r,\varphi).$$

In this equation, $\Phi_{nk}(r) = J_n(\omega_{nk}r) + A_{nk}I_n(\omega_{nk}r)$, where J_n, I_n are the Bessel and Neumann functions of the nth order; A_{nk} is a constant, which is determined by the boundary conditions; ω_{nk} is the natural frequency of the plate oscillations. The expression obtained for the response function provides for both the qualitative and quantitative agreement with the experiment. This is confirmed by data presented in Fig. 2, which shows the experimental response function and that calculated by Eq. (2) for the second electrode of the mirror (the electrode configuration shown in Fig. 1*b*). The experimental and analytically calculated deformation amplitudes amount to 3.18 and 2.97 μm, respectively.

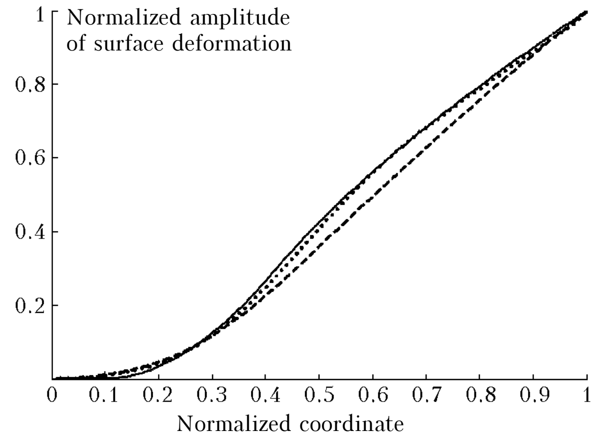

Fig. 2. Response function of the second electrode of the flexible mirror with the electrode configuration as shown in Fig. 1*b*: experimental dependence (solid line); calculation based on the analytical model (dashed line), the relative deviation from the experiment is 0.37%; calculation based on the finite element method (dotted line), the relative deviation from the experiment is 0.022%.

The dotted line in Fig. 2 shows the response function calculated for this electrode by the technique proposed, which is considered below in this paper.

Projection formulation of FEM (FEM-PF)

Despite the existence of the explicit analytical expression for the response function of a given electrode, the numerical solution of Eq. (1) is more efficient. The eigenvalues k_{ns}^2, needed for the calculation of natural oscillation frequencies of the plate, are the solution of a transcendental equation and their calculation is very computationally expensive. However, the numerical solution of Eq. (1) by ordinary numerical methods, for example, the finite difference method, causes certain difficulties, in particular, when finding the second derivative of a discontinuous function in the right-hand side of the equation. The FEM-PF is a method for solution of differential equations in an arbitrary domain with the boundary conditions of a certain form,[6,7] and it allows these difficulties to be avoided.

It is most efficient when solving the Laplace equation with the Neumann boundary conditions.[8] In the case of the central symmetry of the problem (for electrodes in the form of concentric rings and the free fixing of the mirror) and in the static case, Eq. (1) can be reduced to two Laplace equations, and the boundary conditions (1a) and (1b) can be reduced to the Neumann conditions through the following substitution:

$$U(r) = \nabla^2 W(r), \quad f(r) = \frac{d_{31} a^2 E_1 (2\Delta_1 h_1 - h_1^2)}{D2(1-\nu)} E_{\text{el}}(r). \quad (3)$$

Then the equations to be solved take the form:

$$\nabla^2 U(r) = \nabla^2 f(r) \quad (4)$$

with the boundary condition

$$\frac{\partial U}{\partial r} = 0 \text{ at } r = 1; \quad (4a)$$

$$\nabla^2 W(r) = U(r) \quad (5)$$

with the boundary condition

$$\frac{\partial W(r)}{\partial r} = -\frac{1}{\nu - 1} U(r), \quad (5a)$$

where $W(r)$ is the surface profile of the mirror; $U(r)$ is the function describing the surface curvature; $f(r)$ is the dimensionless strength of the field acting in the piezoceramics. These equations involve the dimensionless coordinate $r = \rho/a$, normalized to the plate radius a.

The solution of Eq. (4) is determined accurate to a constant, which can be found from the condition of existence of the solution to Eq. (5):

$$U(r) = U(r) + C,$$

$$C = \frac{1}{\pi(2\nu - 1)} \left(\iint\limits_{\text{circle}} U \, d\sigma - \nu \int\limits_0^{2\pi} U \, d\varphi \right).$$

To solve these equations by the FEM-PF method, we used the FastFlo 3.0 program package, which allows the solution of the equation of mirror deformation. With the use of 400 points for the radius of calculation, the computation on PC AMD 1700 228 Mb RAM takes less than 1 s.

The results of numerical simulation of a flexible five-electrode mirror with electrodes in the form of concentric rings (the electrode configuration shown in Fig. 1*b*) with the use of FEM-PF are presented. Figure 2 depicts the response functions for the second ring. Table 1 summarizes the relative deviations of the calculated response functions from the experimental ones for each electrode, as well as the deformation amplitudes of the experimental and calculated response functions. From Fig. 2 and Table 1, one can see a good qualitative and quantitative agreement between the experimental and calculated response functions. The difference between the calculated and experimental deformation amplitudes of the mirror falls within the measurement uncertainty, which also confirms good accuracy provided by the model.

Variational formulation of the finite element method (FEM-VF)

However, the projection approach does not allow the problem to be solved in the general form at an arbitrary electrode configuration. Its application is limited to the assumption that the mirror is a thin plate. However, the actual reflecting surface of the mirror can be spherical, and, for convenience of mounting, the substrate radius is usually longer than the ceramics radius. In addition, in the analytical model of the mirror it is assumed that the Poisson coefficients of the substrate and ceramics are the same. However, for the widely used PKR-7 piezoceramics and the LK-105 mirror,[9] they amount to 0.34 and 0.17, respectively. Neither in the analytical model nor in the FEM-PF it is possible to dispose of these assumptions.

The numerical model developed by us on the basis of FEM-VF accounts for all the design features of the mirror mentioned above. In addition, this method is more promising, because its further development will allow us to dispose of the approximate theory of deformation of thin plates. FEM-VF is a method of reduction of the problem with infinite number of unknowns (mirror displacement at any point) to the equations, connecting a finite number of parameters, determining approximately the sought surface profile of the mirror.

Table 1. Comparison of experimental and calculated response functions of the five-electrode mirror

Electrode number	1	2	3	4	5
Amplitude of the experimental response function, μm	1.76 ± 0.11	3.18 ± 0.11	3.3 ± 0.11	3.4 ± 0.11	2.7 ± 0.11
Amplitude of the calculated response function, μm	1.75 ± 0.11	3.06 ± 0.11	3.15 ± 0.11	3.33 ± 0.11	2.81 ± 0.11
Relative deviation, %	$5.5 \cdot 10^{-2}$	$2.2 \cdot 10^{-2}$	$1.3 \cdot 10^{-2}$	$3.9 \cdot 10^{-2}$	$2.8 \cdot 10^{-2}$

In accordance with the finite element method,[10] the region under study is divided into finite elements of a simple shape, which are assumed to interact only at a limited number of nodal points. The equations, connecting the nodal parameters, can be derived from the condition of equilibrium of an individual element and have the form

$$S^i = R^i Z^i + P^i, \tag{6}$$

where

$$R = \int_V B^T DB \, \mathrm{d}V \cdot Z \tag{7}$$

is the reaction matrix of the element;

$$P = -\int_V B^T f \, \mathrm{d}V$$

is the reaction vector of the element; S^i is a column vector of forces, arising at the element nodes, if the element deformation is described by the vector of nodal displacements Z^i, and the element is under the action of the nodal forces, described by the reaction vector of the element P^i, which appear due to piezoelectric stresses. The nodal displacements of every element Z^i are connected with the surface profile $z(r,\varphi)$ of the deformed element as: $z(r,\varphi) = N(r,\varphi)Z$, where $N(r,\varphi)$ is the row vector of the shape functions, which are presented in Table 2 in the normal coordinates L_i, related to the Cartesian coordinates in the plate plane (x,y) by the following relationships:

$$\begin{pmatrix} L_1 \\ L_2 \\ L_3 \end{pmatrix} = \frac{1}{2A} \begin{pmatrix} k_1 & y_{23} & x_{32} \\ k_1 & y_{23} & x_{32} \\ k_1 & y_{23} & x_{32} \end{pmatrix} \begin{pmatrix} 1 \\ x \\ y \end{pmatrix},$$

$$2A = x_{13}y_{23} - y_{13}x_{23}, \; k_i = e_{ijk}x_j y_k, \; x,y_{ij} = x,y_i - x,y_j,$$

where x_i, y_i are the coordinates of the element apexes, the indices i, j take the values from 1 to 3.

Table 2

Row vector	Shape function
N_1	$L_1(1 + L_1L_2 + L_1L_3 - L_2^2 - L_3^2)$
N_2	$-y_{12}(L_1^2L_2 + 0.5L_1L_2L_3) + y_{31}(L_1^2L_3 + 0.5L_1L_2L_3)$
N_2	$-x_{21}(L_1^2L_2 + 0.5L_1L_2L_3) + x_{13}(L_1^2L_3 + 0.5L_1L_2L_3)$
N_1	$L_2(1 + L_2L_3 + L_1L_2 - L_1^2 - L_3^2)$
N_5	$-y_{23}(L_2^2L_3 + 0.5L_1L_2L_3) + y_{12}(L_2^2L_1 + 0.5L_1L_2L_3)$
N_6	$-x_{32}(L_2^2L_3 + 0.5L_1L_2L_3) + x_{21}(L_2^2L_1 + 0.5L_1L_2L_3)$
N_7	$L_3(1 + L_3L_2 + L_3L_1 - L_2^2 - L_1^2)$
N_8	$-y_{31}(L_3^2L_1 + 0.5L_1L_2L_3) + y_{23}(L_3^2L_2 + 0.5L_1L_2L_3)$
N_9	$-x_{31}(L_3^2L_1 + 0.5L_1L_2L_3) + x_{23}(L_3^2L_2 + 0.5L_1L_2L_3)$

The stiffness matrix $B = LN$ in Eq. (7) can be found through differentiation of the shape functions

$$L^T = -z\left[\frac{\partial^2}{\partial x^2} \frac{\partial^2}{\partial y^2} \frac{2\partial^2}{\partial x \partial y}\right],$$

the matrix

$$D = \int_{-\Delta_1}^{\Delta_2} \frac{z^2 E}{1-\nu^2} \begin{bmatrix} 1 & \nu & 0 \\ \nu & 1 & 0 \\ 0 & 0 & \frac{1-\nu}{2} \end{bmatrix} \mathrm{d}z,$$

the integral is calculated over the element thickness (coordinate z). Note that the material parameters E and ν can depend on z.

The ultimate equation for displacements of all nodes follow from the condition of equilibrium of the plate as a set of elements. In the case of a free boundary, it follows from this condition that the actions of the elements S^i at any node should be mutually compensated: $\sum_i S_j^i = 0$, the summation is performed over all elements, including the node j. This procedure was realized in Mathlab 6.0. For the numerical simulation, we have selected a flexible mirror with the electrode configuration shown in Fig. 1*c*. Figure 3 shows the experimental (*a*) and calculated (*b*) response functions of the electrode belonging to the middle ring (18th electrode).

One can see a good agreement between the numerically simulated and experimentally measured response functions. The quantitative agreement between the calculated and experimental response functions is confirmed by Fig. 4, which shows the contributions of the Zernike polynomials to the experimental and calculated response functions.

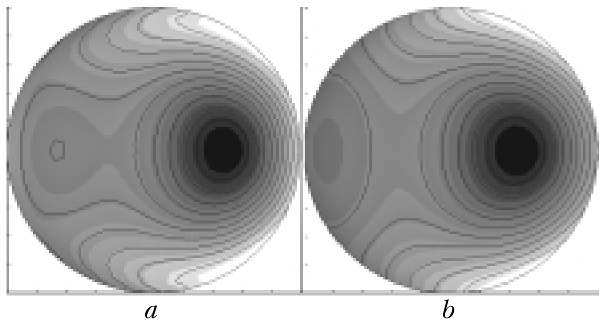

Fig. 3. Experimental response function of the second-ring electrode (18th electrode) (*a*) and calculated response function of the second-ring electrode (*b*). The relative deviation is 7.7%.

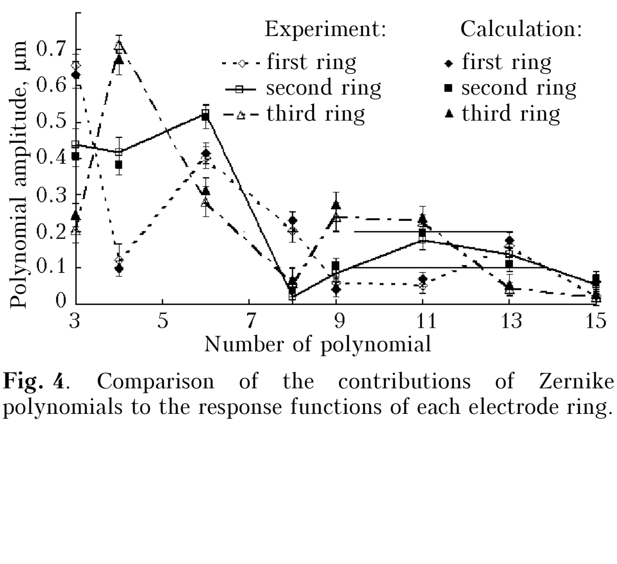

Fig. 4. Comparison of the contributions of Zernike polynomials to the response functions of each electrode ring.

Tilts are subtracted, and therefore the numeration begins from the third polynomial. The differences between the experimental and calculated response functions (see Figs. 3 and 4) can be explained by the fact that real mounting of the mirror is not, strictly speaking, absolutely free. In addition, we also ignored the effect of glue, changing the interaction between the substrate and ceramics. However, as can be seen from Fig. 4, the differences between the experimental and calculated response functions are within the measurement and calculation errors, which confirms quite good accuracy of the model.

Conclusions

The two numerical models of a semi-passive mirror, developed on the basis of the two approaches of the finite element method, have been described and analyzed comparatively. The projection algorithm, based on the solution of the equation describing the deformation of a thin plate, is simple and the computer program based on it is highly efficient, but it is applicable only for the central symmetry. The variational approach, based on the equations for a plate as a set of finite elements, is not so efficient, but it is applicable in the case of arbitrarily shaped electrodes of the mirror. The comparison with the experimental results has demonstrated quite good accuracy of both models: the deviation of the theoretical response functions from the experimental ones falls within the measurement error. In the course of this work, a refined equation has been obtained for the analytical description of the electrode response function. This equation provides for not only qualitative, but also quantitative agreement with the experimental data.

Acknowledgments

This work has been done within the framework of the ISTC Project No. 2631 "Adaptive optical system for phase correction of laser beams with screw-type wave front dislocations."

References

1. T.Yu. Cherezova, L.N. Kaptzov, and A.V. Kudryashov, Appl. Opt. **35**, No. 15, 2554–2561 (1996).
2. A.V. Kudryashov and V.V. Samarkin, Opt. Commun. **118**, No. 5, 317–322 (1995).
3. S.A. Kokorovsky, J. Opt. Soc. Am. **69**, No. 1, 181–187 (1979).
4. A.V. Kudryashov and V.I. Shmalhausen, Opt. Eng. **35**, No. 11, 3064–3073 (1996).
5. M.A. Vorontsov, A.V. Kudryashov, and V.I. Shmalhausen, Izv. Vyssh. Uchebn. Zaved., Fizika **27**, No. 11, 1419–1430 (1984).
6. O.C. Zienkiewicz and K. Morgan, *Finite Elements and Approximation* (J. Wiley & Sons, New York, 1983), 328 pp.
7. L.J. Segerlind, *Applied Finite Element Analysis* (J. Wiley & Sons, New York, 1976).
8. V.E. Shmelev, *Partial Differential Equations Toolbox*; http://www.matlab.ru/pde/book1/index.asp.
9. V.V. Samarkin, *"Development and investigation of adaptive bimorph mirrors to control the radiation of serial* CO_2 *and high-power femtosecond lasers*", Cand. Dissert., Moscow (2002), 159 pp.
10. A.S. Volkov and V.E. Bobushev, *Bending Analysis of Plates by the Finite Element Method* (Khabarovsk, 1996), 67 pp.